ISSN 1808-8546 (ONLINE) 1808-3765 (CD-ROM)

DETECÇÃO SEMI-AUTOMÁTICA DE ÁRVORES EM POMAR DE MANGUEIRA IRRIGADA A PARTIR DE IMAGENS OBTIDAS POR DRONE

CARLOS ANDRÉ DE SOUZA SÁ[1]; MAGNA SOELMA BESERRA DE MOURA[2]; JOSICLÊDA DOMICIANO GALVÍNCIO[3]; RODRIGO DE QUEIROGA MIRANDA[3]; MARCELO JOSÉ DA SILVA[4] E CLOVES VILAS BOAS DOS SANTOS[3]

[1] Programa de Pós Graduação em Engenharia Agrícola, Universidade Federal do Vale do São Francisco, Av. Antônio Carlos Magalhães, 510, Santo Antônio, CEP 48903-210, Juazeiro, BA, Brasil, carlosandreagronomia@outlook.com.
[2] Embrapa Semiárido, BR 428, Km 152, s/n, Zona Rural, Petrolina, PE, Brasil, magna.moura@embrapa.br.
[3] Programa de Pós Graduação em Desenvolvimento e Meio Ambiente, Universidade Federal de Pernambuco, Av. Acadêmico Hélio Ramos, s/n, Cidade Universitária, 50.740-530, Recife, PE, Brasil, josicleda@hotmail.com, rodrigo.qmiranda@gmail.com, clovesvilasboas@gmail.com.
[4] Programa de Pós Graduação em Engenharia Agrícola, Universidade Federal Rural de Pernambuco, Rua Manuel de Medeiros, s/n, Dois Irmãos, CEP 52.071-000, Recife, PE, Brasil, marcelosilvaagr@gmail.com.

1 RESUMO

O monitoramento da população de plantas em áreas agrícolas é fundamental para acompanhar a produtividade, auxiliar no planejamento e na tomada de decisão. Assim, objetivou-se propor um protocolo para identificação remota de árvores de mangueiras no Submédio do Vale São Francisco por meio de *softwares* e *plugins* gratuitos aplicados em imagens aéreas obtidas com drones. O estudo foi desenvolvido em três pomares de mangueira, empregando-se modelos digitais obtidos a partir de ortomosaicos gerados em três qualidades de processamento; avaliados no QGIS utilizando-se os *plugins* '*Tree Density Calculator*' e 'SAGA GIS'. Os resultados obtidos foram avaliados por meio dos índices de Precisão, Revocação e F1–*Score*. O índice de Precisão foi mais elevado para o processamento em qualidade baixa. O índice de Revocação apresentou maiores valores no processamento em qualidade média e elevada, indicando que quanto maior a qualidade do processamento, maior é a chance de acertar na contagem de árvores. Os maiores valores de F1–*Score* foram observados para o *Tree Density Calculator* com processamento na resolução baixa. Recomenda-se o uso de um protocolo para a identificação e contagem remota de árvores de mangueiras, de forma semi-automática por meio da utilização de imagens obtidas por VANTs e *softwares* de código livre e aberto.

Palavras-chave: Identificação de árvores, mangicultura, sensoriamento remoto, veículo aéreo não tripulado.

SÁ, C. A. S.; MOURA, M. S. B.; GALVÍNCIO, J. D.; MIRANDA, R. Q.; SILVA, M. J.; SANTOS, C. V. B.
SEMI-AUTOMATIC DETECTION OF TREES IN IRRIGATED MANGO ORCHARD FROM IMAGES OBTAINED BY DRONE

Recebido em 25/01/2021 e aprovado para publicação em 03/11/2021
DOI: http://dx.doi.org/10.15809/irriga.2021v26n3p507-524

2 ABSTRACT

The monitoring of plant populations in agricultural areas is essential to follow the productivity, assisting in planning and decision making. Thus, our objective was to propose a protocol for remote detection of mango trees in the *Low-Middle of the Sao Francisco River* Valley, by using free software and plugins applied on aerial drone images. The study was conducted in three mango orchards. We used digital models extracted from orthomosaics created under three level of quality; then they were evaluated on the package QGIS with the plugins 'Tree Density Calculator' and 'SAGA GIS'. The results were evaluated with the indices Precision, Recall and F1–Score. The precision index was higher for low-quality processing; while the recall index showed higher values under medium and high quality, indicating that the higher the quality of the processing, the greater is the chance of acquiring an efficient tree counting. The highest F1–Score values were observed for the Tree Density Calculator plugin with low processing resolution. We recommend using this protocol for the remote identification and counting of mango trees, in a semi-automatic methodology by using aerial images obtained using UAVs and free software and plugins.

Keywords: Identification of trees, mango cultivation, remote sensing, unmanned aerial vehicle.

3 INTRODUCTION

Brazil stands out for its high production of agricultural products, which is due mainly to favorable soil and climate conditions and public and private investments in research, technology, and infrastructure to maximize production (PASSOS; FONTES; NASCIMENTO, 2020). Among the most economically exploited fruit trees in Brazil, the mango tree *Mangifera indica* L. stands out, making the country the seventh largest producer in the world (FOOD AND AGRICULTURE ORGANIZATION OF THE UNITED NATIONS, 2019), surpassed only by India, Indonesia, China, Mexico, Pakistan, and Malawi. According to data from the Brazilian Institute of Geography and Statistics (IBGE)/SIDRA, total mango production in Brazil in 2020 was 1,569,011 tons, with an emphasis on the Tommy Atkins, Keitt, Kent, and Palmer cultivars, which are the main contributors to Brazilian exports. In the same year, the Northeast Region accounted for the majority of Brazilian production, accounting for approximately 1,230,995 tons, with an emphasis on Pernambuco, the country's largest producing state, which contributed 624,611 tons of fruit (BRAZILIAN INSTITUTE OF GEOGRAPHY AND STATISTICS, 2021). Despite the water and soil (structure, texture, and nutrient) restrictions found in part of the interior of Northeast China (AMARAL, 2011), the Submiddle São Francisco Valley region, located in the central portion of the Brazilian semiarid region, has shown the highest productivity rates, exporting approximately 87% of the mangoes produced in Brazil.

With the expansion of agricultural areas, information on the exact number of fruit trees is essential for both estimating plant survival rates and monitoring their productivity (LI et al., 2017; MASCHLER; ATZBERGER; IMMITZER, 2018) and is even useful for calculating carbon stocks (ZHANG, 2019). Vegetation detection and quantification have several purposes, including obtaining information on plant health (BARNES et al., 2017) and assessing vegetation related to indirect parameters, such as the percentage of green cover (HERNÁNDEZ-HERNÁNDEZ et al., 2016), among others, such as nutritional and

water status, which together aid in decision-making within the farm. Furthermore, the generation of georeferenced data on orchards is extremely useful for the development of Agriculture 4.0.

Typically, plant counting is performed manually by rural workers. Despite its effectiveness in terms of identification, this method is quite inefficient because of the high demand for man-hours (ABIDIN et al., 2017). Remote sensing, in turn, is an important alternative for automating the plant counting process by acquiring information without direct contact with the targets, using high spatial resolution images (LI et al., 2017). In this sense, to improve the quality of cultivated area surveys, the use of unmanned aerial vehicles (UAVs) is an important alternative because it provides aerial remote sensing data with high temporal and spatial resolutions and at lower costs for coverage of small- and medium-sized areas than traditional aerial platforms do.

Through the use of UAVs, it is possible to acquire georeferenced crop data, depending on the type of sensor used. Furthermore, different parts of the electromagnetic spectrum can be explored via digital image processing (PÁDUA et al., 2020). According to this same author, georeferenced images can be used to calculate orthorectified results through photogrammetric processing, such as orthophoto mosaics, digital elevation models (DEMs), spectral indices, and various byproducts of digital processing.

The success of identifying and quantifying a set of fruit trees depends on the spatial resolution of the image; the dominance of the tree within the orchard in terms of overlap, crown union, branch separation, and target geometry; the terrain topography; and especially the type of sensor used in the image acquisition process (OJEDA-MAGAÑA et al., 2020). All of these factors can facilitate or hinder tree counting.

The process of analyzing digital images is quite complex, especially in regard to detecting vegetation, given its morphometric parameters, which typically vary under natural conditions. Ojeda-Magaña et al. (2020), seeking to automatically detect oak trees, reported that the size, shape, and color of vegetation, as well as the edge of the tree canopy in contrast to ground images and its own shadow, are factors that directly interfere with the correct identification of trees. The authors explained that individual detection is hampered precisely by the difficulty in delimiting the region of each tree, whether when a tree's shadow is projected onto itself or onto the ground where the tree canopy and shadows have similar colors or even when a tree canopy has multiple regions.

According to Arantes et al. (2020), there is no single specific methodology for vegetation identification and the validation of results; rather, several studies have used remote sensing. In this sense, different techniques and methods are available to identify trees and their elements or even metric parameters (e.g., crown diameter and plant height). However, comparative analysis becomes difficult because of the need for reference data and evaluation metrics (LI et al., 2016). This is because some methods are based on spectral classes, detection neural networks, deep learning, and algorithms for self-organizing data analysis techniques. On the other hand, tree detection results can also be validated simply by comparing them with manual results, as reported by Wagner et al. (2018) and Weinstein et al. (2019). However, these methodologies are not accessible to most users, mainly because of the requirement for advanced scientific knowledge and the use of machines with greater execution capacity.

With these considerations in mind, the aim is to propose a protocol for the remote identification and counting of mango trees in the Sub-Middle São Francisco Valley via free *software* and *plugins* applied

to aerial images obtained with drones, thus providing information for an agricultural analysis of the orchard.

4 MATERIALS AND METHODS

The study was carried out in three mango orchards, two commercial and one research area (Figure 1), located in the municipality of Petrolina, Pernambuco, Sub-Middle São Francisco Valley. According to the Koppen classification, the region has a Bswh' climate type (semiarid), with a rainy season between January and April (ÁLVARES et al., 2013).

Figure 1. Locations of commercial and experimental mango orchards in Petrolina-PE.

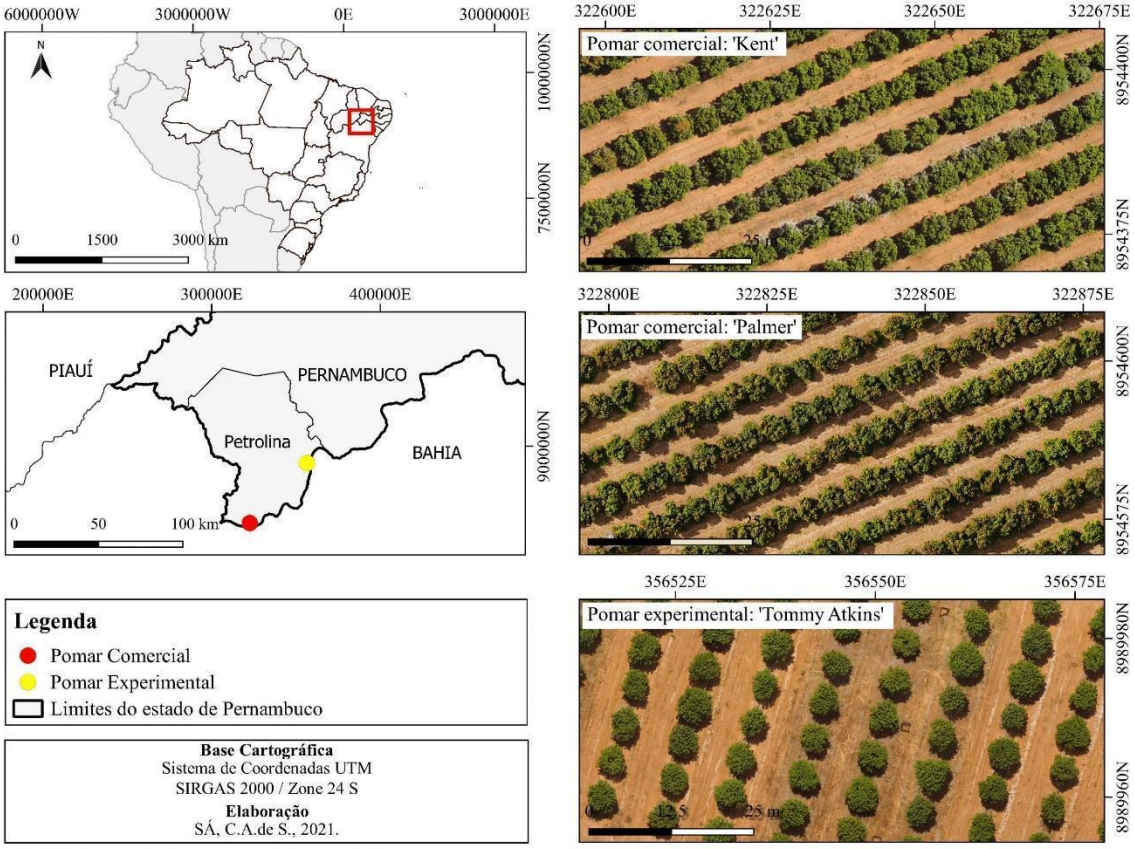

Source: Authors (2021).

The three orchards used for this study have mango cultivars 'Kent' and 'Palmer' (commercial orchards) and 'Tommy Atkins' (experimental orchard), whose planting information is shown in Table 1. The soils of commercial areas are classified as sandy (SANTOS et al., 2006), whereas the experimental soils present a medium-clayey texture (BRANDÃO et al., 2017).

Table 1. Characteristics of mango orchards.

Mango cultivar	Area (ha)	Spacing (m)
Kent	3.54	4 x 7
Palmer	4.00	4 x 7
Tommy Atkins	0,86	5 x 8

Source: Autores (2021).

To obtain the images, flights were carried out via the commercial drone DJI Phanto m 3 Standard (DJI PHANTOM, 2021a) in the orchards of the Kent and Tommy Atkins cultivars and the DJI Phanto m 4 Pro v2 drone (DJI PHANTOM, 2021b) for the area planted with the Palmer cultivar. The first drone was equipped with a 1/2.3" 12 Mp CMOS sensor, FOV 94° 20 mm (35 mm equivalent format) and f/2.8 aperture, and the second drone was equipped with a 1" 20 Mp CMOS sensor, FOV 84° 8.8 mm/24 mm (35 mm equivalent format) and f/2.8-f/11 aperture. The aircraft were used according to availability at the time of the flights. Both are registered according to Brazilian standards, and the flight plans were carried out in compliance with legislation, with flights at an altitude of 80 m to cover a larger area per battery and at an altitude of 50 m in the Tommy Atkins orchard (experimental area). An 80% lateral and frontal overlap was adopted to ensure that the orthomosaic was closed, and the camera was positioned at a 90-degree angle to the drone, pointing directly at the ground, with the camera set to manual mode according to the scene's lighting.

The captured images were processed via the trial version of Agisoft Metashape Professional Edition 1.5.2® software, generating a digital surface model (DSM), a digital terrain model (DTM), and an orthomosaic. The first step in image processing is the generation of digital products (Figure 2), of which the orthomosaic, DTM, and DTM are essential for tree detection in this study. However, depending on the variable analyzed, the quality of the processing can affect the results. According to Hyslop et al. (2020), three types of digital models can be obtained by processing images acquired by satellites or UAVs: the digital elevation model (DEM), which captures elevation as well as the plant canopy; the digital terrain model (DTM), which captures elevation on the basis of the terrain, ignoring elevations above ground; and the digital surface model (DSM), which captures all elevations above ground (such as buildings, streets, trees, etc.). The outcome of these products depends on several factors, including the resolution, frontal and side overlap of the photographs, brightness, and altitude of the UAV used to collect the images, as well as the *image processing quality of the software*. Thus, the images for each mango orchard were processed in three processing qualities: low (B), medium (M), and high (E). Finally, the *software itself* generates a report detailing the generated products. This report includes information about the camera used, the products generated, and their resolution and is measured via the *ground sample distance* (GSD) . The GSD represents the image pixel in the terrain units and is associated with the final processing quality through the level of detail of the aerial survey. The value given by the GSD is inversely proportional to the level of detail; that is, the higher the GSD is, the lower the level of detail, and vice versa.

Figure 2. Image processing steps were performed with a UAV in a mango orchard to generate digital products via Agisoft Metashape® *software*.

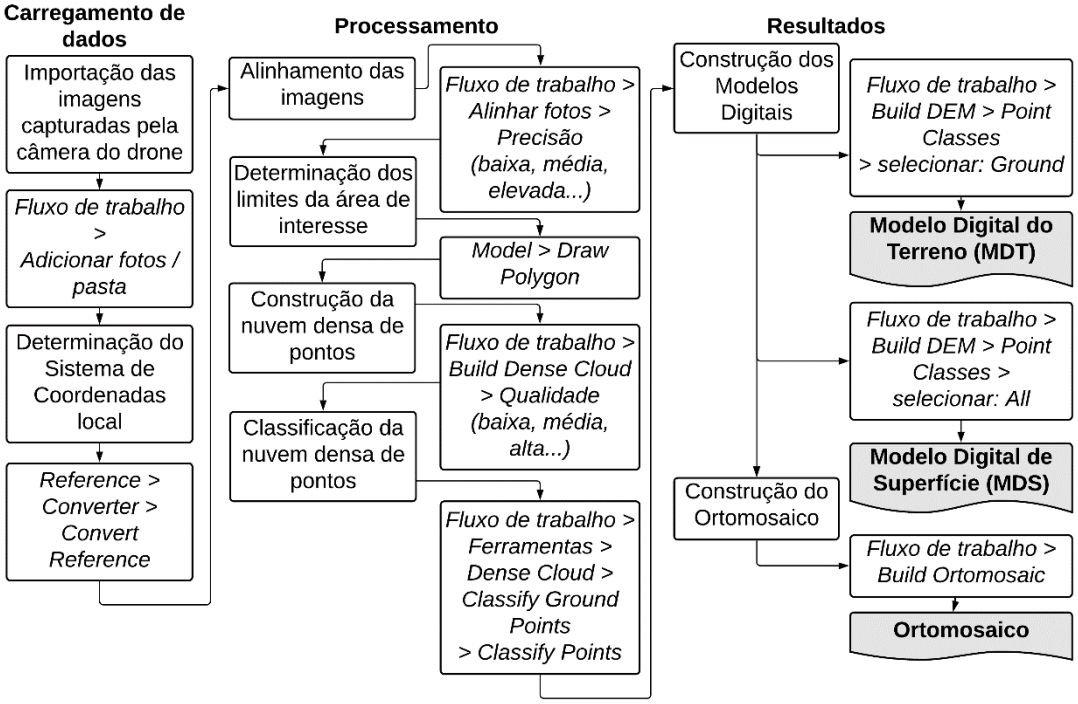

Source: Authors (2021).

After the products (digital models and orthomosaics) of all the imaged areas were generated, they were cropped to delimit the areas of interest in the orchard. This cropping is necessary to eliminate objects that are not of interest to the study and that are generally located around the area of interest, such as buildings, vehicles, reservoirs, people, and other points considered to be elevations, so that these do not interfere with the generation of the DSM and DTM. The digital height model (DHM) was generated by subtracting the DSM from the DTM, for which QGIS® was used. To achieve this, a *shape* (file) with the boundaries of the area to be studied was first created, and using the *Raster tool*, cropping was performed on the *mask layer* (files with the area boundaries). The resulting product was the same digital model but was now cropped to the study area. The MDH was generated via the ' *Raster* ' tool, which uses the ' *Raster* Calculator', the cropped MDS and MDT files, and the equation: *MDH = MDS - MDT*. The orthomosaic was subsequently cropped, which was necessary for manual tree counting. This count is essential for validating the results and is also a requirement for the automated counting process.

To carry out this study, QGIS *software* version 3.10.8-A Coruña® was used, and the *plugins were tested. Tree Density Calculator* version 1.5.7 (CRABBÉ et al., 2020) and the SAGA *System for Automated Geoscientific Analyses* version 2.3.2 (CONRAD et al., 2015), both free and easy-to-use, were evaluated for their ability to count mango trees.

After generating, cropping and preparing the digital products, processing was carried out to identify the trees *via 'tree' plugins. Density'* (from MDH) and 'SAGA' (from MDS and MDT), generating two files with the detected points, one for each plugin, here referred to as ' *shape* points' (Figure 3). Next, each tree present in all the orchards was identified and manually counted to compare the results obtained automatically with those obtained manually. On the basis

of the calculation of the plant population, taking into account crop spacing, the theoretical and actual stands were compared, in addition to checking the number of missing trees in each orchard.

Figure 3. Processing steps of digital products obtained from UAV images for *shape point generation* and mango tree detection.

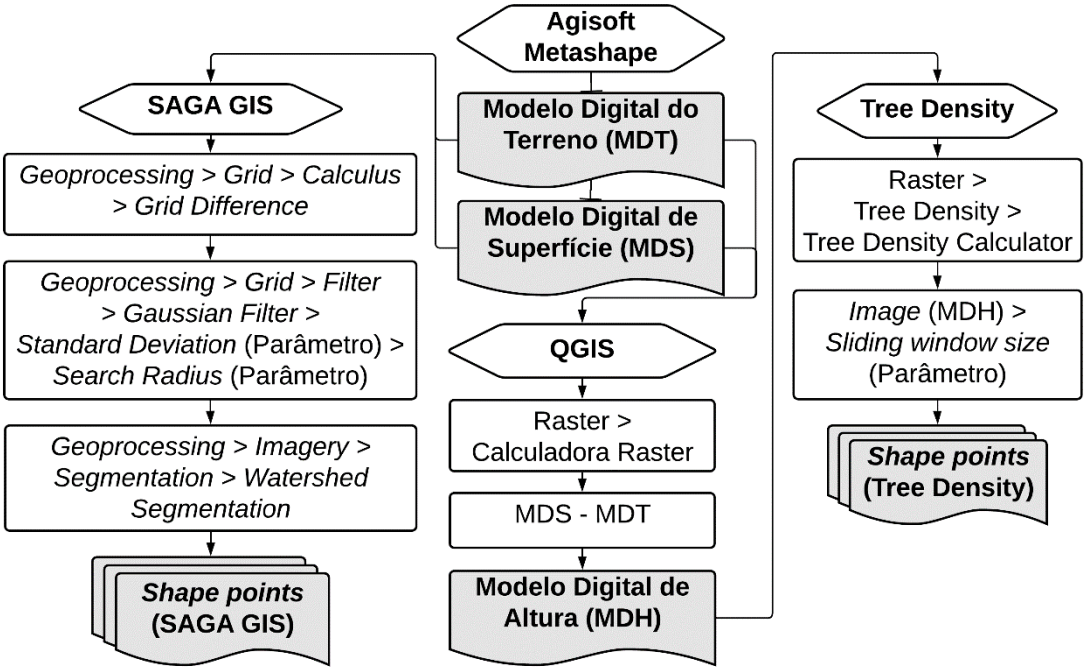

Source: Authors (2021).

The potential of each technique, which is based on processing quality (low, medium, and high), *plugins* (SAGA and *tree density*), and cultivars ('Kent', 'Palmer', and 'Tommy Atkins'), was evaluated via the Precision (Equation 1), Recall (Equation 2), and F1-*Score* (Equation 3) indices. The detected trees, incorrect points, and undetected trees correspond to the numbers of true positives (TPs), false positives (FPs), and false negatives (FNs), respectively, in a contingency table. Statistical differences between the mean orthomosaic *ground sample distance* and DEM values across study areas and processing qualities were assessed via *one-way analysis of variance (ANOVA)*. All the statistical analyses were performed via the R package v3.5.3 (R CORE TEAM, 2020).

$$\text{Accuracy} = VP/(VP + FP) \quad (01)$$

$$\text{Recall} = VP/(VP + FN) \quad (02)$$

$$F1\text{–}\textit{Score} = 2 * (\text{Precision} * \text{Recall})/(\text{Precision} + \text{Recall}) \quad (03)$$

5 RESULTS AND DISCUSSION

The orthomosaics and digital models resulting from the processing of images captured from the mango orchards of the 'Kent', 'Palmer', and 'Tommy Atkins' cultivars are shown in Figures 4, 5, and 6, respectively. The orthomosaics in Figures

4A and 5A present the trees in a very similar way, as both flights were conducted at an altitude of 80 m, even though different aircraft were used (Phantom 3 and Phantom 4, respectively). In turn, as shown in Figure 6A, the plants are larger in size, precisely due to the flight altitude of 50 m. These characteristics resulted in significant differences in pixel size between the orchards, with the largest GSD of the orthomosaic being observed in the orchard of the Kent cultivar, followed by 'Tommy Atkins' and 'Palmer' (Table 2), implying differences in the resolution of the orthomosaics. On the other hand, no significant difference ($p < 0.05$) was detected when the images were processed at low, medium, or high quality, regardless of the orchard analyzed (Table 2). In practice, when the same equipment (computer or notebook) is considered, performing all the processing steps (Figure 2) at different quality levels implies different processing times. The time required to obtain the final products at low resolution is shorter than that at medium resolution and, in turn, shorter than that at high resolution. Therefore, this is an important step when agility in the delivery of digital products is required when contracting services on agricultural property.

Figure 4. Digital products obtained from the processing of aerial images obtained by a UAV for the 'Kent' mango orchard: A) orthomosaic; B) digital terrain model (DTM); C) digital surface model (DSM); and D) digital height model (MDH).

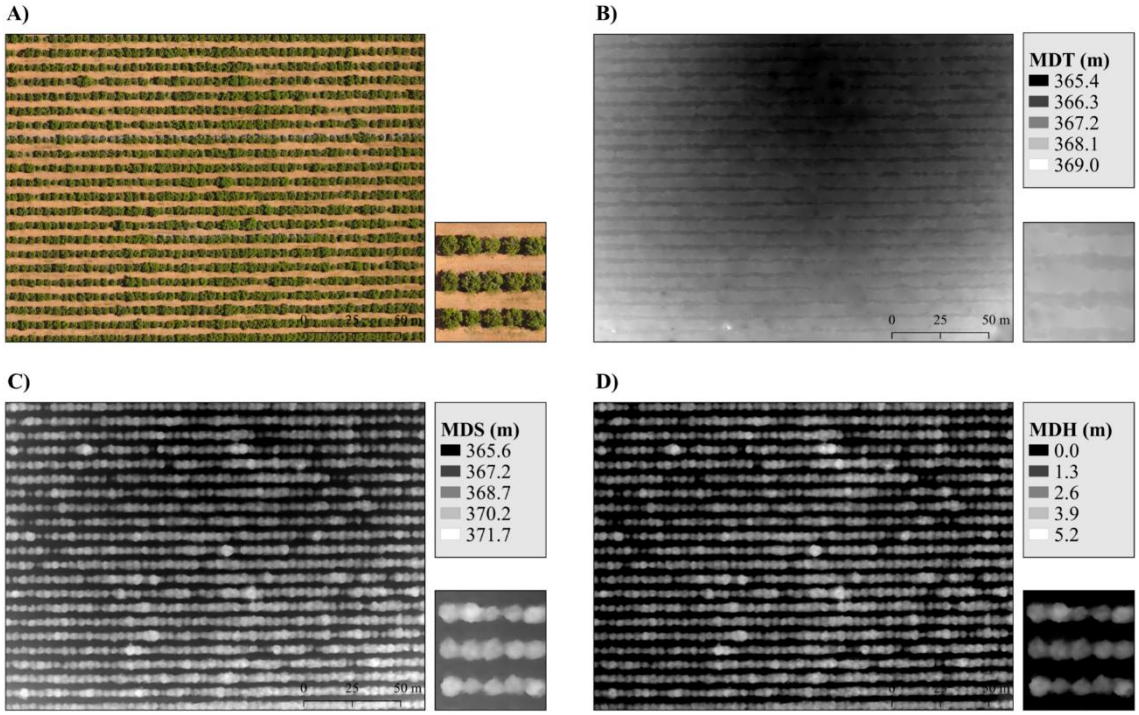

Source: Authors (2021).

Figure 5. Digital products obtained from the processing of aerial images obtained by a UAV for the 'Palmer' mango orchard: A) orthomosaic; B) digital terrain model (DTM); C) digital surface model (DSM); and D) digital height model (MDH).

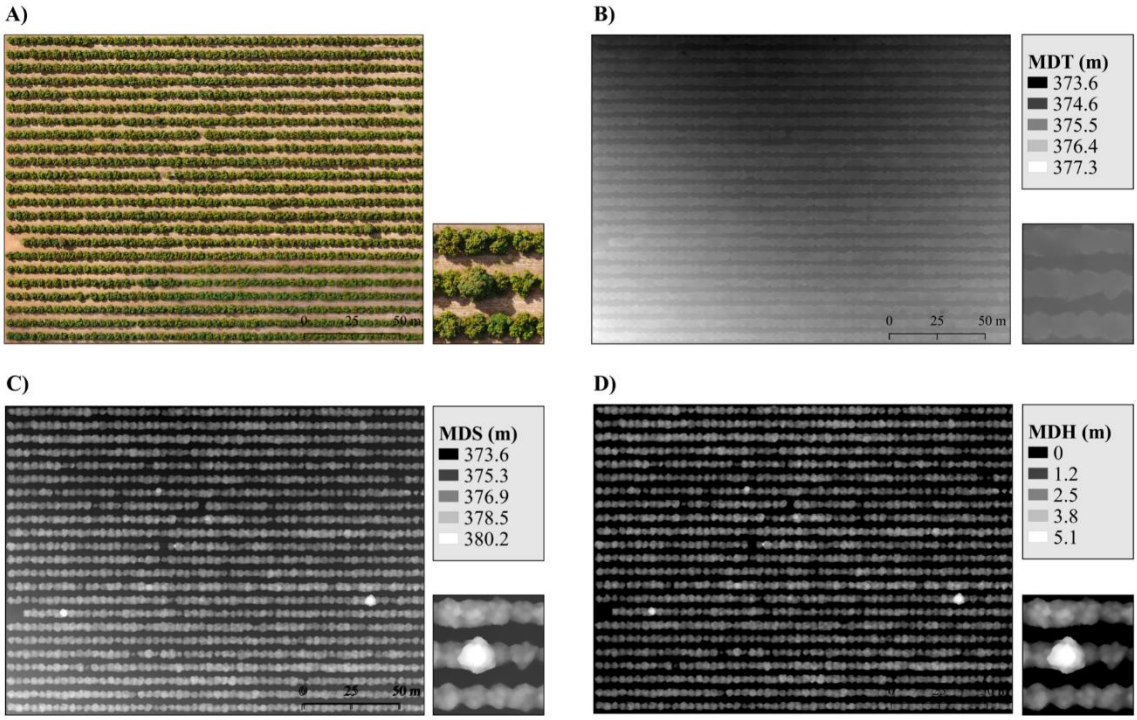

Source: Authors (2021).

Figure 6. Digital products obtained from the processing of aerial images obtained by a UAV for the 'Tommy Atkins' mango orchard: A) orthomosaic; B) digital terrain model (DTM); C) digital surface model (DSM); and D) digital height model (DHM).

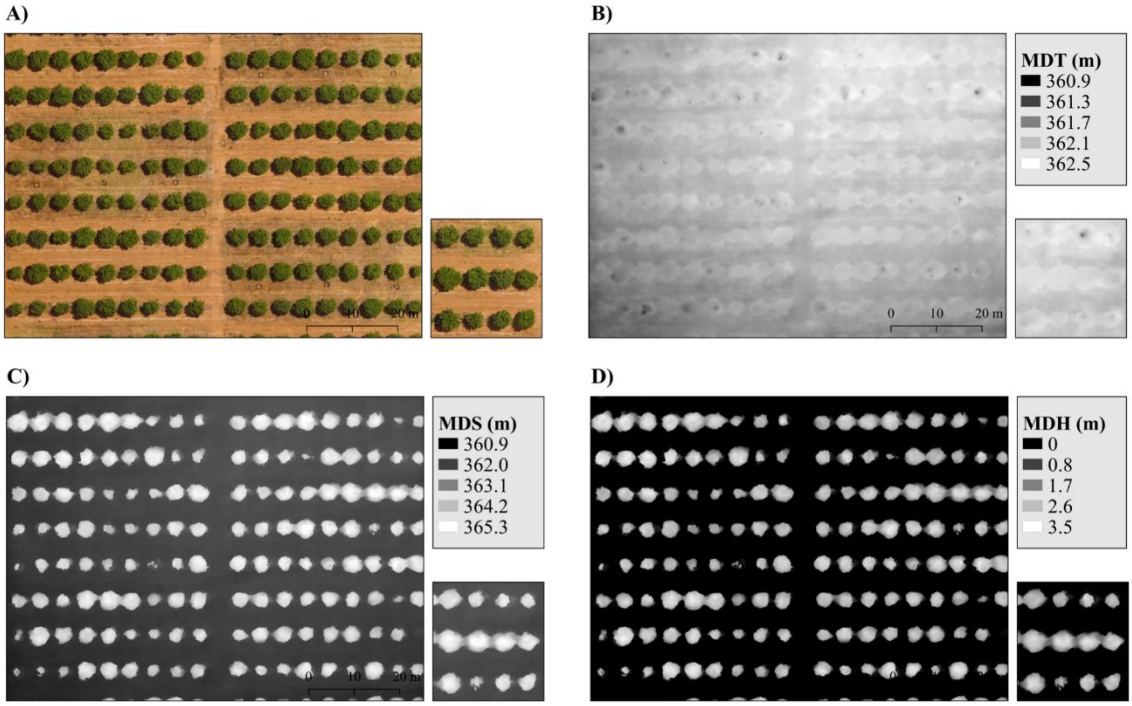

Source: Authors (2021).

Table 2. Pixel resolution of the orthomosaic and digital surface model (DSM) obtained from processing different UAV image qualities.

Cultivar implanted	Area (ha)	Processing Quality	Orthomosaic GSD (cm/pixel)	GSD of the MDS (cm/pixel)
Kent	3.54	Low	$3,07^{aA}$	$24,6^{aA}$
		Média	$3,06^{aA}$	$12,2^{aB}$
		Elevada	$3,07^{aA}$	$6,15^{aC}$
Palmer	4,00	Baixa	$2,12^{cA}$	$17,0^{aA}$
		Média	$2,11^{cA}$	$8,45^{aB}$
		Elevada	$2,11^{cA}$	$4,22^{aC}$
Tommy Atkins	0,86	Baixa	$2,58^{bA}$	20.7^{aA}
		Average	2.60^{bA}	10.4^{aB}
		High	2.61^{bA}	5.22^{BC}

Note: Different lowercase letters (a, b, c) indicate significant differences ($p < 0.05$) between different areas, whereas different uppercase letters (A, B, C) are related to different processing qualities. GSD: Ground sample distance.

Source: Authors (2021).

The digital terrain (DTM), surface (DSM), and height (DHM) models are shown in Figures 4 to 6 (B, C, and D, respectively). The DTM shows that the ground level difference is small for the 3.54 ha area of the 'Kent' orchard (Figure 4B), as well as for the 4.0 ha orchard of the 'Palmer' cultivar (Figure 5B). These two areas are relatively close and have similar topographic characteristics. However, regarding the tree

size of both cultivars, the 'Palmer' plants (Figure 5D) were smaller than the 'Kent' plants (Figure 4D), a characteristic observed through DHM. In the case of 'Palmer', there are few taller trees, which stand out for their white color (Figure 5D), with heights of approximately 5.1 m, whereas in the 'Kent' orchard, the number of taller trees is much greater (Figure 4D). Because it is a commercial mango orchard, the taller trees in the 'Palmer' orchard come from a planting error with the 'Espada' mango variety.

The GSD associated with the digital models did not significantly differ between the orchards. However, the processing quality (low, medium, and high) resulted in different digital model qualities (Table 2). The highest values were observed, in decreasing order, in the low-, medium-, and high-quality models, almost doubling between them. This implies that the higher processing quality resulted in higher resolution of the digital models, which quantitatively presented many more points.

When the digital images obtained from the 'Tommy Atkins' orchard were analyzed, greater detail and uniformity of the tree canopy were noted (Figure 6A). The DTM also shows that the terrain slope is almost negligible for the orchard's area of approximately 0.86 ha. Since this is an experimental area, the plants are more spaced (Table 1), and the flight in this area was conducted at an altitude of 50 m, allowing the orthomosaic and digital images to be generated with a lower GSD.

According to Arantes et al. (2020), orthomosaics with well-spaced plant crowns facilitate the semiautomatic identification of each individual. In general, high-resolution aerial images over small areas enable clearer analysis of tree crown dimensions, as well as the correct identification of each individual plant's canopy. For this reason, the digital products of the Tommy Atkins orchard, especially the orthomosaic, allow for a more detailed analysis of the field's plant canopy.

When the digital models were constructed, negative values were observed for the MDH of all the orchards (Figures 4D, 5D, and 6D). Upon noticing this same behavior, Morte, Carvalho, and Barros (2020) explained that even though negative values are close to zero, which occurs due to overestimations of the relief altitude, despite being rare, they can interfere with the calculation of the average height of the tree canopy, since these values would be included in the soil sections. Therefore, to reduce this noise, the authors recommend the application of filters to eliminate values below zero, thus generating digital height models with greater accuracy.

After generating the digital products, a manual count of the trees in each orchard was performed to validate the automatic detection results obtained by the *plugins*, as per Wagner et al. (2018) and Weinstein et al. (2019). Manual counting was performed in the field to verify the results, and in the QGIS *software*, the orthomosaic was used as the digital product, generating a *shapepoint file for comparison with the plugin* results. In this process, points are added one by one to each visually identified tree. This technique is not classified as the most efficient among the other methods, mainly because it requires more time and attention from the operator to avoid errors of omission or addition in the visual interpretation process.

Figure 7 presents the results of the manual tree count, totaling 1,265 trees in the 'Kent' mango orchard, 1,423 trees in the 'Palmer' orchard, and 215 trees in the 'Tommy Atkins' mango orchard. On the basis of the calculation of the plant stand for each area and the visual analysis of the orthomosaics, two missing trees were detected in the 'Palmer' mango orchard, and one missing tree was detected in the 'Tommy Atkins' orchard. These results were compared with the outputs of the *plugins* tested in each orchard using the digital products at different resolutions.

Figure 7. Identification tree manual for each orchard: A) 'Kent' mango orchard with 1,265 trees identified; B) 'Palmer' mango orchard with 1,423 trees present and two missing trees identified; C) 'Tommy Atkins' mango orchard with 215 trees present and one missing tree identified.

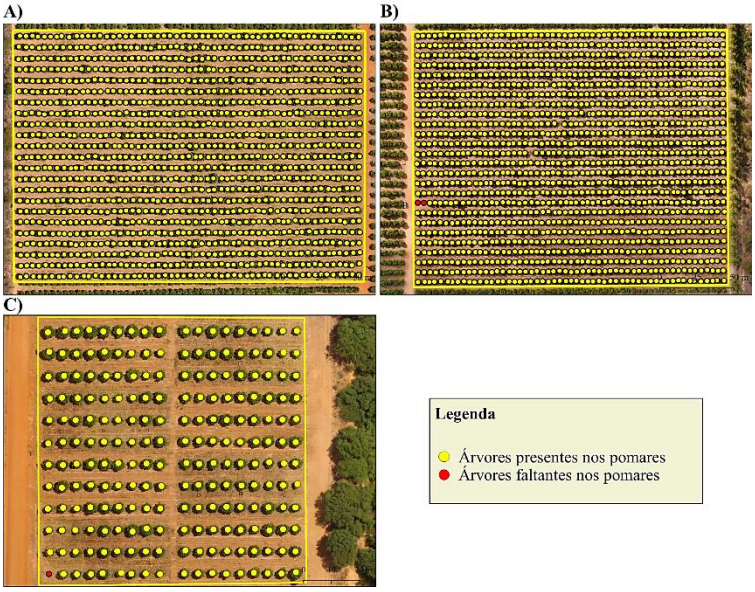

Source: Authors (2021).

In the 'Kent' orchard, the best result for semiautomatic tree detection was achieved through high-quality processing and the use of the SAGA GIS *plugin*, resulting in 1,251 correctly detected trees, equivalent to 98.9% of the actual stand (Figure 8), leaving only 14 missing trees. However, the total numbers of detected points and incorrect objects with this same procedure were 1,563,070 and 1,561,819, respectively. This result allows us to observe that the viability of tree identification is not associated only with processing quality because although this choice generated the highest percentage of correct answers, many points that did not represent trees were also identified, requiring more time for the operator to eliminate incorrectly detected points. In other words, correct detection represents the identification of the highest pixel identified in the tree canopy (FREI TAS, 2021). Other authors also obtained similar results for individual counting, such as Isip et al. (2018), who obtained an accuracy of 88.89% when counting mango trees with well-spaced canopies via algorithms for tree detection.

Quality processing via the *Tree Density plugin*, which is ranked as the fourth-best treatment for semiautomatic tree detection, yielded significant results by incorrectly detecting only one object, although it identified 750 trees in the Kent orchard, equivalent to 59.3% (Figure 8) of the actual stand, and 515 missing trees. This was the processing method that resulted in the fewest incorrectly identified objects.

High-quality processing with the SAGA GIS plugin for the 'Palmer' orchard resulted in the identification of 100% of the trees in the orchard (Figure 8), that is, 1,426 trees, a significantly greater percentage than that obtained through processing performed with the *Tree Density plugin*. However, as observed in the 'Kent' orchard, the number of detected points (6,377,445 points) and incorrectly detected objects (6,376,019 points) is significantly greater than the actual value (1,426 trees). With respect to the use of SAGA GIS, processing at medium and low quality obtained different results, although both have the same characteristic

of detecting many incorrect objects: most of the points clustered at the edges of the images, and the remainder were on top of trees with interconnected canopies. The results obtained in the 'Palmer' orchard via the *Tree Density plugin* did not differ significantly in processing quality, a behavior similar to that observed with the same treatment applied to the 'Kent' orchard. Adopting this *plugin* enabled us to obtain information about the plant stand in a timelier manner for this orchard, as obtaining high-quality digital models requires much more time than processing at low quality. The *Tree Density plugin* yielded satisfactory results regardless of processing quality.

With respect to the results obtained in the 'Tommy Atkins' orchard (Figure 8), the processing performed at medium and high qualities allowed the detection of 100% of the trees when SAGA GIS was used and 98.6% with *tree density*, with 215 and 212 trees identified, respectively. The results obtained from processing at low quality and using the *tree density plugin* were less efficient, identifying only 95 trees.

Figure 8. Percentages of trees correctly detected (recall) via SAGA GIS and *tree density plugins* for processing with low (B), medium (M) and high (E) qualities in mango orchards of the Kent (K), Palmer (P) and Tommy Atkins (T) cultivars in Petrolina, PE.

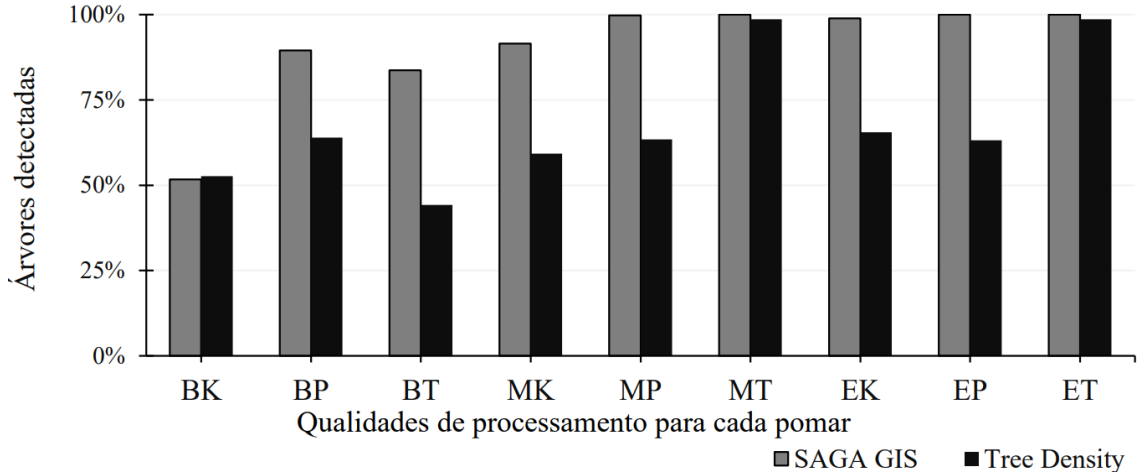

Source: Authors (2021).

Table 3 presents the values for precision, recall, and the F1 *score* for the treatments analyzed. The precision index was highest for low-quality processing, regardless of the cultivar and *plugin* evaluated, whereas the recall index showed higher values for medium- and high-quality processing, indicating that the higher the processing quality was, the greater the chance of accurate tree counting, since the digital models obtained had higher point density. For this index (recall), the best results were obtained with the SAGA GIS *plugin* (Table 3). In a previous study that shared some of the methodologies proposed in this research, Gonçalves et al. (2019) achieved better detection when evaluating invasive species via the SAGA GIS plugin. For *plugin* selection, the F1 *score, which combines both precision and revolution in a single index,* was considered. Thus, in the present study, the highest average F1 *score values* were observed for the *Tree Density plugin* with low-resolution processing. In fact, in practice, this treatment allows greater operationalization for technical use, being indicated for use in counting irrigated mango

trees in the Sub-Middle São Francisco Valley.

Table 3. Precision, recall and F1-*score* indices for evaluating the *plugin* and the quality of processing of UAV images obtained from mango orchards in the Sub-Middle São Francisco Valley.

Plugin	**Cultivate**	**Quality**	**Precision**	**Revocation**	**F1– *Score***
SAGA GIS	Kent	Low	0.970	0.517	0.675
		Average	0.449	0.915	0.602
		High	0.001	0.989	0.002
	Palmer	Low	0,700	0,895	0,785
		Média	0,004	0,998	0,008
		Elevada	0,000	1,000	0,000
	Tommy Atkins	Baixa	0,184	0,837	0,301
		Média	0,001	1,000	0,003
		Elevada	0,000	1,000	0,000
Tree Density	Kent	Baixa	0,991	0,526	0,688
		Média	0,999	0,593	0,744
		Elevada	0,654	0,655	0,655
	Palmer	Baixa	0,997	0,640	0,779
		Média	0,516	0,635	0,569
		Elevada	0,091	0,632	0,159
	Tommy Atkins	Baixa	0,168	0,442	0,244
		Média	0,200	0,986	0,332
		High	0.080	0.986	0.149

Source: Authors (2021).

6 CONCLUSIONS

The identification of mango trees via a semiautomatic process using digital products obtained from images of unmanned aerial vehicles (UAVs) and the use of *plugin tree density* and SAGA GIS were similarly possible through digital processing performed at low, medium, and high quality. Therefore, owing to the shorter time required to achieve the final products, low-quality processing is recommended, especially for technology companies focused on agriculture, which need to deliver results to the client in a relatively shorter timeframe.

The *Tree Density* and SAGA GIS plugins performed best for tree detection in the 'Kent' mango orchard, which has a relatively large cultivated area and large trees, demonstrating that these *plugins* can be used in orchards of varying sizes. Among the *plugins*, the 'tree density calculator' performed best for semiautomatic mango tree detection and is the most recommended, as it yields the highest number of correct results and requires less manual intervention to obtain the final results.

This article presents a protocol for semiautomatic remote identification and counting of mango trees via aerial images obtained via UAVs, free *software*, and *plugins.* Similarly, given the efficiency observed in this study, we recommend that this protocol be evaluated for the detection of trees of other crop species.

7 ACKNOWLEDGMENTS

The authors are grateful for the support provided by the Embrapa ET-VANT Project (20.18.04.003.00.00). Carlos AS Sá thanks the Bahia Research Support Foundation (FAPESB) for a Master's scholarship (BOL 0724/2020). Josicleda D. Galvíncio thanks the National Council for Scientific and Technological Development (CNPq) for the research productivity scholarship (PQ 302934/2018-9) and for the funding of the Universal Project process 402834/2016-0. Rodrigo Q. Miranda thanks the Pernambuco Science and Technology Support Foundation (FACEPE) for processing APQ 0646-9.25/16.

8 REFERENCES

ABIDIN, H.; SAMAD, MN; PING, LY; NOOR, MKAM Evaluation of recognition software for oil palm tree counting under different planting conditions and ages. *In* : INTERNATIONAL CONFERENCE ON BIG DATA APPLICATIONS IN AGRICULTURE, 11., 2017, Serdang. **From Nursery to Field** . Serdang: Institute of Plantation Studies, 2017. v. 1, p. 124-133.

ÁLVARES, CA; STAPE, JL; SENTELHAS, PC; GONÇALVES, JL de M.; SPAROVEK, G. Köppen's climate classification map for Brazil. **Meteorologische Zeitschrift** , Berlin, v. 22, no. 6, p. 711-728, 2013.

AMARAL, FCS **Brazilian Land Classification System for Irrigation** : focus on the semiarid region. Rio de Janeiro : Embrapa Solos, 2011.

ARANTES, B. H. T.; ARANTES, L. T.; SANTOS, J. M.; VENTURA, M. V. A.; GOMES, L. F. Efficiency analysis of the use of model matching algorithm for plant counting. **Research, Society and Development**, Vargem Grande Paulista, v. 9, n. 7, p. e668974576, 2020.

BARNES, C.; BALZTER, H.; BARRETT, K.; EDDY, J.; MILNER, S.; SUÁREZ, J. C. Individual tree crown delineation from airborne laser scanning for diseased larch forest stands. **Remote Sensing**, Basel, v. 9, n. 3, p. 231, 2017. DOI: https://doi.org/10.3390/rs9030231. Disponível em: https://www.mdpi.com/2072-4292/9/3/231. Acesso em: 29 abr. 2021.

BRANDÃO, S. da S.; GIONGO, V.; OLSZEVSKI, N.; SALVIANO, AM Vegetable cocktails and management systems altering soil quality and mango productivity. **Brazilian Journal of Physical Geography** , Recife, v. 10, n. 4, p. 1079-1089, 2017.

CRABBÉ, AH; CAHY, T.; SOMERS, B.; VERBEKE, LP; VAN COILLIE, F. **Tree Density Calculator Software.** Version 1. 5.3. Ghent: Laboratory of Forest Management and Spatial Information Techniques, 2020. Available at: https://bitbucket.org/kul-reseco/localmaxfilter. Accessed on: April 4, 2020.

CONRAD, O.; BECHTEL, B.; BOCK, M.; DIETRICH, H.; FISCHER, E.; GERLITZ, L.; WEHBERG, J.; WICHMANN, V.; BOHNER, J. System for Automated Geoscientific Analyzes (SAGA) v. 2.1. 4. **Geoscientific Model Development** , Gottingen, v. 8, n. 7, p.

1991-2007, 2015. DOI: https://doi.org/10.5194/gmd-8-1991-2015. Available at: https://gmd.copernicus.org/articles/8/1991/2015/. Accessed on: February 10, 2021.

DJI PHANTOM. Specifications: Phantom 3 Standard. Consumer Page. Available at: https://www.dji.com/br/phantom-3-standard. Accessed on: April 27, 2021a.

DJI PHANTOM. Specifications: Phantom 4 Pro V2.0. Consumption Page. Available at: https://www.dji.com/br/phantom-4-pro-v2/specs. Accessed on: April 27, 2021b.

FAO. FAOSTAT 2019. Available at: http://www.fao.org/faostat/en/#data/. Accessed on: January 18, 2022.

DRONE SHOW. **Automatic tree counting in images obtained with drones** . Curitiba: Mundo GEO, 2021. Available at: https://droneshowla.com/contagem-automatica- dearvores-em-imagens-obtidas-com-drones/. Accessed on: May 10, 2021.

GONÇALVES, J.; PÔÇAS, I.; MARCOS, B.; MÜCHER, CA; HONRADO, JP SegOptim - A new R package for optimizing object-based image analyzes of high-spatial resolution remotely sensed data. **International Journal of Applied Earth Observation and Geoinformation** , Enschede , v. 76, p. 218-230, 2019. DOI: https://doi.org/10.1016/j.jag.2018.11.011. Available at: https://www.sciencedirect.com/science/article/abs/pii/S0303243418303556. Accessed on: May 12, 2021.

HERNÁNDEZ-HERNÁNDEZ, J.; GARCÍA-MATEOS, G.; GONZÁLEZ-ESQUIVA, J.; ESCARABAJAL HENAREJOS , D.; RUIZ-CANALES, A.; MOLINA-MARTÍNEZ, J. Optimal color space selection method for plant/soil segmentation in agriculture. **Computers and Electronics in Agriculture** , Amsterdam , v. 122 , p. 124-132, 2016. DOI: https://doi.org/10.1016/j.compag.2016.01.020. Available at: https://www.sciencedirect.com/science/article/abs/pii/S0168169916000259?via%3Dihub. Accessed on: February 11, 2021.

HYSLOP, K.; GALDINO, S.; QUARTAROLI, CF; ZOLIN, CA; TOSTO, SG Evaluation of different Digital Surface Models (DSM) in the delimitation of the Piririm River basin-AP using the Invest software. *In* : INTERINSTITUTIONAL CONGRESS OF SCIENTIFIC INITIATION, 14., 2020, Campinas. **Proceedings** [...]. Campinas: Embrapa Agricultural Informatics, 2020.

IBGE. **Municipal agricultural production 2020** . Table 1613. Brasília, DF: SIDRA, 2020. Available at: https://sidra.ibge.gov.br/tabela/1613. Accessed: January 17, 2022.

ISIP, M. F.; CAMASO, E. E.; DAMIAN, G. B.; ALBERTO, R. T. Estimation of Mango Tree Count and Crown Cover Delineation using Template Matching Algorithm. **International Journal for Research in Applied Science and Engineering Technology**, [s.l.], v. 6, n. 3, p. 1955-1960, 2018.

LI, Y.; CAO, Z.; LU, H.; XIAO, Y.; ZHU, Y.; CREMERS, A. B. In-field cotton detection via region-based semantic image segmentation. **Computers and Electronics in Agriculture**, Amsterdam, v. 127, p. 475-486, 2016. DOI: https://doi.org/10.1016/j.compag.2016.07.006.

Disponível em: https://www.sciencedirect.com/science/article/abs/pii/S016816991630480X. Acesso em: 17 fev. 2021.

LI, W.; FU, H.; YU, L.; CRACKNELL, A. Deep learning based oil palm tree detection and counting for high-resolution remote sensing images. **Remote Sensing**, Basel, v. 9, n. 1, p. 22-35, 2017. DOI: https://doi.org/10.3390/rs9010022. Disponível em: https://www.mdpi.com/2072-4292/9/1/22. Acesso em: 17 fev. 2021.

MASCHLER, J.; ATZBERGER, C.; IMMITZER, M. Individual Tree Crown Segmentation and Classification of 13 Tree Species Using Airborne Hyperspectral Data. **Remote Sensing**, Basel, v. 10, n. 8, p. 1218-1247, 2018. DOI: https://doi.org/10.3390/rs10081218. Disponível em: https://www.mdpi.com/2072-4292/10/8/1218. Acesso em: 03 mai. 2021.

MORTE, CLB; CARVALHO, LFSG; BARROS, RS Use of UAV as a tool for canopy height estimation in mangroves: an investigative study in Guaratiba, Rio de Janeiro, Brazil. **Tamoios Journal** , São Gonçalo , v. 16, n. 3, p. 42-51 , 2020. DOI: https://doi.org/10.12957/tamoios.2020.55745. Available at: https://www.e-publicacoes.uerj.br/index.php/tamoios/article/view/55745. Accessed on: May 6, 2021

OJEDA-MAGAÑAA, B.; RUELAS, R.; QUINTANILLA-DOMÍNGUEZ, J.; GÓMEZ-BARBA, L.; LÓPEZ DE HERRERA, J.; ROBLEDO-HERNÁNDEZ, J.G.; TARQUIS, A.M. Automatic identification of the area covered by acorn trees in the dehesa (pastureland) Extremadura of Spain. **Computers and Electronics in Agriculture** , Amsterdam , v. 172, p. 105289-105298, 2020. DOI: https://doi.org/10.1016/j.compag.2020.105289. Available at: https://www.sciencedirect.com/science/article/abs/pii/S0168169919318526. Accessed on: February 10, 2021.

PÁDUA, L.; ADÃO, T.; SOUSA, A.; PERES, E.; SOUSA, J.J. Individual grapevine analysis in a multitemporal context using UAV-based multisensor imagery. **Remote Sensing** , Basel, v. 12, n. 1, p. 139-160, 2020. DOI: https://doi.org/10.3390/rs12010139. Available at: https://www.mdpi.com/2072-4292/12/1/139. Accessed on: February 10, 2021.

data envelopment analysis model. **Revista Custos e Agroneg ocio online** . Recife , v. 16, special issue, p. 105-141, 2020.

R CORE TEAM. **The R Project for Statistical Computing** . Vienna: R Core Team, 2020. Available at: www.r-project.org/. Accessed on: April 30, 2021.
SANTOS, HG; JACOMINE, PKT; ANJOS, LHC; OLIVEIRA, VA; OLIVEIRA, JB; COELHO, MR; LUMBRERAS, JF; CUNHA, TJF (ed.). **Brazilian soil classification system** . 2nd ed. Rio de Janeiro: Embrapa Soils, 2006.

WAGNER, FH; FERREIRA, MP; SANCHEZ, A.; HIRYE, MC; ZORTEA, M.; GLOOR, E.; PHILLIPS, OL; SOUZA FILHO, CR; SHIMABUKURO, YE; ARAGAO, L. E. Individual tree crown delineation in a highly diverse tropical forest using very high-resolution satellite images. **ISPRS Journal of Photogrammetry and Remote Sensing** , Amsterdam , v. 145, p. 362-377, 2018. DOI: https://doi.org/10.1016/j.isprsjprs.2018.09.013. Available at: https://www.sciencedirect.com/science/article/pii/S0924271618302582. Accessed on: February 10, 2021

WEINSTEIN, B. G.; MARCONI, S.; BOHLMAN, S.; ZARE, A.; WHITE, E. Individual tree-crown detection in RGB imagery using semisupervised deep learning neural networks. **Remote Sensing**, Basel, v. 11, n. 11, p. 1309-1322, 2019. DOI: https://doi.org/10.3390/rs11111309. Disponível em: https://www.mdpi.com/2072-4292/11/11/1309. Acesso em: 06 mai. 2021.

ZHANG, X. Quick Aboveground Carbon Stock Estimation of Densely Planted Shrubs by Using Point Cloud Derived from Unmanned Aerial Vehicle. **Remote Sensing** , Basel, v. 11, no. 24, p. 2914- 2932 , 2019. DOI: https://doi.org/10.3390/rs11242914. Available at: https://www.mdpi.com/2072-4292/11/24/2914. Accessed on: 29 April. 2021.